QUANTITATIVE EVALUATION OF EARTHQUAKE-DAMAGED RC PIERS

(Translation from Proceedings of JSCE, No. 648/V-47, May 2000)

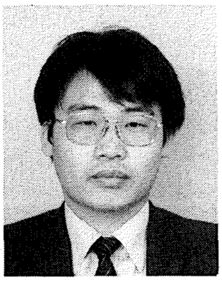


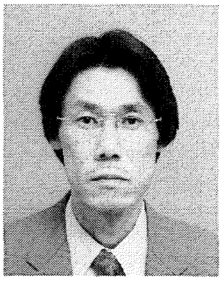

Kenji KOSA　　Hideki SONE　　Tsunekazu NAKATA　　Mikio TASAKA

To evaluate the relationship between the damage level and the ultimate bearing capacity of piers, a quantitative investigation was conducted on the RC single piers along the Hanshin Expressway Kobe Route, which were severely affected by the 1995 Hyogo-ken Nambu Earthquake. According to the results of the investigation, 72 piers ranked As and A (severest damage and severe damage, respectively) and had termination of reinforcement at the column mid-height were all damaged at the termination point. Their average shear strength index was smaller than the index of piers ranked B1 or below. There were also 11 piers ranked As and A that were damaged at the column mid-height, even though their reinforcement was not terminated at that point. These piers were found to have a shear strength vs. flexural strength ratio of below 1 and an extremely small shear strength index.

Keywords: seismic resistance, ductility, failure mechanism, termination of reinforcement

---

Kenji KOSA, a member of the JSCE and the ASCE, is an associate professor in the Department of Civil Engineering at the Kyushu Institute of Technology. Before joining the faculty in 1999, he was a senior highway engineer at the Hanshin Expressway Public Corporation. He obtained his Ph.D. from the University of Michigan in 1988. His main research interests are the design and analysis of concrete structures.

Hideki SONE is a Director of the Kyoto Construction Division at the Hanshin Expressway Public Corporation. After 30 years since his work for the original construction of the Kobe Route from 1968 to 1970, Sone was again assigned to work for the restoration and reconstruction of the earthquake-damaged Kobe Route from 1995 to 1998. His research interest is the design of steel and concrete structures. He is a member of the JSCE.

Tsunekazu NAKATA is a section manager at Yachiyo Engineering Co., Ltd. He obtained his MS in civil engineering from Kyoto University in 1977. His research interest is the seismic design of concrete structures. He is a registered consulting engineer and a member of the JSCE.

Mikio TASAKA is a deputy manager at the Obayashi Corporation in Tokyo. He obtained his BS in civil engineering from Hokkaido University in 1984. He is a registered PE and a member of the JSCE.

---

1. INTRODUCTION

Tremendous damage was caused to the bridge structures on the Hanshin Expressway Kobe Route when the Hyogo-ken Nambu Earthquake hit the region in 1995. The damage included the falling of girders at several locations. The route, immediately closed to traffic, was reopened 20 months later after the necessary repairs, strengthening, and reconstruction were made.
In a quick survey after the earthquake, the damaged RC piers were grouped into the following damage ranks: As (severest), A, B, C, and D (minor or no damage). The piers were grouped based on the results of visual inspections and analyses of photographs [1]. Of the 943 RC piers inspected, 142 piers or 15% were ranked As and A, severest and severe damage, respectively, and 327 piers or 35% were given ranks of B and C, which represent relatively light damage. Piers ranked As and A were dismantled and new piers reconstructed in their places. Piers ranked B through D were reused after necessary repairs or strengthening. All foundations were reused because they were found to have been virtually unaffected by the earthquake.

Visual inspections may be adequate to assess the damage level of piers and judge the need for repairs, strengthening, or reconstruction in an urgent situation after the earthquake. But to better evaluate the cause of damage and the damage level of those piers, a quantitative investigation should be carried out using detailed damage information on concrete cracking, reinforcement buckling, etc. This is because visual inspections have the following limitations:

1) Most damage to the concrete and significant damage to the reinforcement can be identified from visual inspection of the cracking and falling of the concrete and the exposed main reinforcement below the fallen cover concrete, respectively. But, visual inspections cannot be used to evaluate B- and C- rank buckling damage to the main reinforcement which is not so evident.
2) Visual inspections cannot evaluate damage to a pier below the ground simply because that section is invisible.

In this research, the detailed results of the investigation of the RC single piers ranked B, C, and D were compared with the results of the visual inspection and then used to perform a quantitative evaluation. First, the level of damage level to the concrete and the pier reinforcements, including the quantity of cracked concrete and the length of the buckled portion of the main reinforcement, were measured. Next, the effects of the damage type, the reinforcement termination, and the point of damage on the damage level of the piers were evaluated. As it was found that the damage level of the piers was significantly influenced by the reinforcement termination and the ground conditions, an analysis was performed using parameters such as the position of reinforcement termination and the ground spring.

2. DETAILED DAMAGE ASSESSMENT

Piers ranked B, C, and D in the initial visual inspection right after the earthquake were reassessed in detail, with a focus on the spalling and cracking of the cover concrete and the buckling and bulging of the main reinforcement. Based on the results obtained, the piers were recategorized into ranks of B1, B2, and B3 by the replacement ratio of the outermost main reinforcement due to buckling, and ranks of C1, C2, and D by the severity of spalling and cracking of the concrete:

B1: nearly the entire outer main reinforcement needs replacement because of bulging around the entire circumference of the column.
B2: about 1/2 of the outer main reinforcement needs replacement.
B3: about 1/4 of the outer main reinforcement needs replacement.
C1: part of the main reinforcement is exposed, but there is no bulging of the main reinforcement
C2: main reinforcement is not exposed, but major cracks observed
D: minor cracks or no damage

A detailed damage assessment was not performed on piers ranked B or below, which had been removed due to significant residual tilting. Piers ranked As and A, and hence immediately covered with steel jacketing for safety and then dismantled for reconstruction, were also not included in the assessment.

To minimize the effect of the pier type, only RC single-type piers were selected for investigation. Figure 1 compares the damage ranks of 443 piers as determined by visual inspection and detailed damage assessment. The figure shows that not a few piers previously given a C or D rank were assigned new ranks of B1, B2, or B3. Figure 2 shows the number of the piers whose initial damage ranks were changed to higher ranks as a result of the detailed assessment. 46 C-ranked and 11 D-ranked piers were assigned new ranks of B3 or above. This is primarily because predominant damage in the underground section of the column, which could not be detected by visual inspection, was discovered during the detailed assessment.

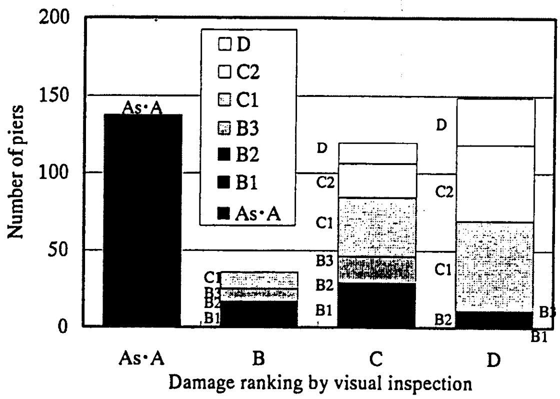

Fig.1 Comparison of damage levels

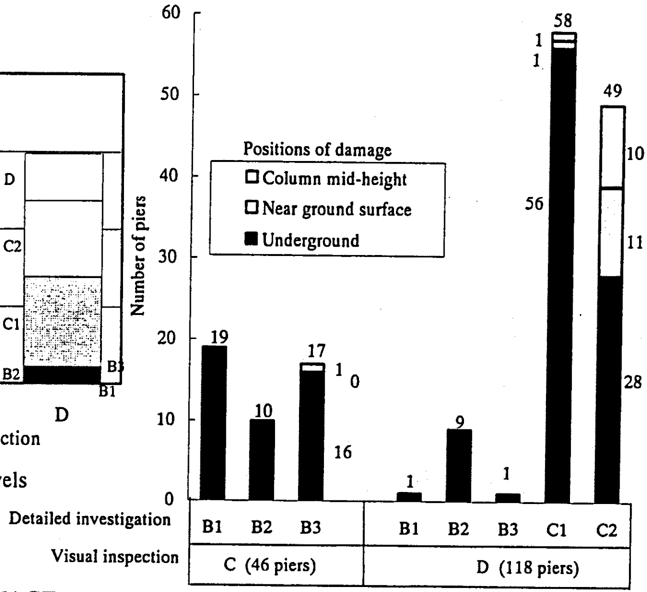

Fig.2 Positions of pier damage

3. QUANTITATIVE ANALYSIS OF DAMAGE

3.1 Assessment of main reinforcement damage

When designing a retrofit for a column, the lengths of the buckling and the bulging of the main reinforcement were used to determine the need to replace the main reinforcement. Here, the length of the buckling means the vertical length of the column where the main reinforcement is bent, and the length of the bulging means the horizontal length from the original position to the apex of the horizontal projection of the main reinforcement. The main reinforcement at the point on the column where the concrete spalled were examined on all piers to determine the need for replacement.

3.2 Length of bulging of the main reinforcement

The length of the bulging of the main reinforcement was measured on about 20 piers selected at random from each pier group for ranks B1, B2, and B3. Table 1 shows the relationship between the damage ranks of the piers and the damage levels of the main reinforcement. Figure 3 shows the relationship between the length of the buckling and the length of the bulging of the main reinforcement.

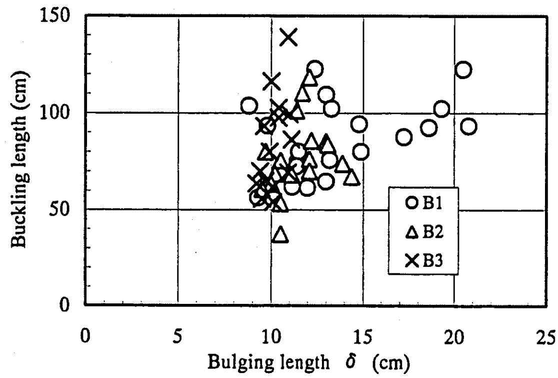

Fig.3 Relationship between bulging length and buckling length of main reinforcement

Table 1 shows good agreement between the damage ranks determined by the detailed assessment and the actual replacement ratio of the main reinforcement, and that the increase in the length of the bulging remained small, from 10 cm to 14 cm, even though the damage rank was increased from B3 to B1. This tendency was probably caused by the process - when the main reinforcement buckled due to loading and an approximately 10 cm of bulge occurred, the resistivity of the main reinforcement to further loading was declined, the load then began to be transferred to the side, and the buckling of the main reinforcement also progressed to that direction. Some piers of B1 rank, the reinforcements of which bulged over 20 cm, were rectangular-shaped piers. The load was probably not as easily transferred to the side on that type of pier as with the circular type.

Table 1 Damage levels of actual bridge piers affected by the earthquake

Damage rank	Concrete chipped	Replacement ratio of outermost main reinforcement	Bulging length of main reinforcement	Buckling length
B1	6.7 m^3	86%	14 cm (4.0D)	88 cm (0.35W)
B2	2.3 m^3	39%	12 cm (3.4D)	77 cm (0.30W)
B3	2.0 m^3	18%	10 cm (2.9D)	84 cm (0.33W)
C1	1.0 m^3	–	–	
C2	0.08 m^3	–	–	
D	0.0 m^3	–	–	

D : D35 is assumed for the main reinforcement
W : width of the cross section

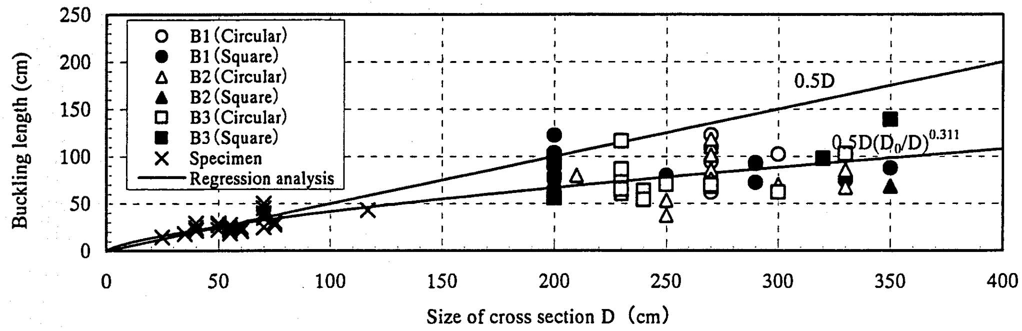

Fig. 4 Relationship between buckling length of main reinforcement and size of column cross section

3.3 Length of buckling of the main reinforcement

Figure 3 indicates that no clear relationship exists between the length of the buckling, which varied widely, from 40 cm to 140 cm, and the assigned damage rank. Figure 4 shows the relationship between the size of the pier cross-section and the length of the buckling in the main reinforcement as measured on specimens and actual bridge piers of ranks B1, B2, and B3. Here, the length of the buckling of the main reinforcement is assumed to be the length of the plastic hinge since the difference between them is relatively small, though the former is, in the strict sense, different from the latter, which is used for calculating the ultimate displacement for the seismic design.

Two lines are described in the figure: one is the line which assumes a length of 0.5D for the plastic hinge, as recommended by past studies; the other line assumes a length of $0.5D\ (D_0/D)^{0.311}$ which is calculated by the "least square" method by taking into account the cross-sectional size of the actual piers. D_0 is assumed to be 55 cm, the average cross-section of the column specimens.

According to Fig. 4, the length of the plastic hinge on an actual bridge pier with a cross-section of over 200 cm tends to be below 0.5D because the length of the buckling of the main reinforcement of this big pier does not increase, even though size of the cross-section is larger. In the case of small piers with a cross-section no greater than 100 cm, the length of the buckling of the main reinforcement increases in proportion to the increase in the size of the cross section [2].

3.4 Analysis of concrete damage

Table 1 shows the amount of the concrete that had chipped from the piers in each damage rank. Here, the chipping range means the range at which the cover concrete fell, or the cracked concrete came apart, as a result of chipping. The amount of chipping from piers of ranks C2 and D was very limited because their damage was simply cracking. In contrast, the chipping amount from piers of ranks B1, B2, and B3 was greater and in proportion to the increase in main reinforcement replacement. For example, in the case of Pier 153 with a square cross-section (3.2 × 3.2 m) and a rank of B3, the ratio of reinforcement replacement was 24%, the length of the buckling was 97.6 cm, the length of the bulging was 10.4 cm, and the amount of chipped concrete was 1.6 m^3 (surface area 9.9 m^2; average depth 0.16 m), indicating that the concrete was chipped up to a level near the main reinforcement.

3.5 Quantitative assessment of damage

The damage levels obtained from 1/6 scale pier specimens and from actual earthquake-damaged bridges on the Kobe Route were compared. The experiment, conducted under reversed loading conditions, was intended to confirm that earthquake-damaged concrete piers could be reused if necessary repairs or strengthening was applied. The details of the experiment are given in Reference 3. The cross-section of the specimens was a 60 × 60 cm square. D10 reinforcing bars were arranged with a spacing of 80 mm as the main reinforcement, and D6 reinforcing bars with a spacing of 200 mm as the hoop ties. The cover concrete was applied to a depth of 40 mm.

The specimens were loaded until they reach damage levels of A, B, and C ranks. The specimen intended to simulate A-rank damage was loaded to a displacement of 7 δ_y (a displacement far exceeding the ultimate displacement) at which all the reinforcements on all four sides buckled. The specimen simulating B-rank damage was loaded to 5 δ_y (nearly equal to the ultimate displacement) at which the main reinforcements on two sides began to bulge and the core concrete began to fail. Specimen C was loaded to 3 δ_y, a displacement at which no buckling of the main reinforcement is expected.

Table 2 shows the damage levels of the specimens. As to the specimen loaded to an A-rank damage level, the ratio of reinforcement replacement was 100 % and the length of the bulging was 4.0D. For the specimen of B-rank damage, the former ratio was 70% and the latter length was 2.5D. In contrast, the average reinforcement replacement ratio for actual piers of ranks B1, B2, and B3 was 47% and the average length of the bulging was 3.4D, as seen in Table 1. In other words, in terms of the replacement ratio of the main reinforcement, the average value of actual piers of ranks B1, B2, and B3 roughly equals the value of specimens of B rank or below. And, in terms of the length of the bulging, the average value for actual piers of the same ranks falls somewhere in between the value of specimens of ranks A and B. Therefore, it can be said that B-rank damage to actual piers is roughly in agreement with B-rank damage to the specimens, which means that actual piers were subjected to earthquake loading that caused an ultimate displacement (approximately 5 δ_y). As actual piers with C-rank damage showed slight damage to the concrete and no buckling of the reinforcement, it roughly corresponds to C-rank damage to the specimens (a displacement of 3 δ_y).

Table 2 Damage levels of specimens

Damage rank	Concrete chipped	Replacement ratio of outermost main reinforcement	Bulging length of main reinforcement
A	0.24 m^3	100%	40 mm (4.0D)
B	0.10 m^3	70%	25 mm (2.5D)
C	—	—	0

Table 3 Typical cracking damages of piers

Pier No.	Inclination angle of cracks (°)	Width of cracks (mm)	Spacing between cracks (cm)
Kobe P-82	65	0.4	17.1
Kobe P-216	70	0.95	16.0
Kobe P-269	59	0.61	17.1

4. ANALYSIS OF DAMAGE TYPES

4.1 Characteristics of shear damage

The number of piers that were damaged by shearing during the earthquake was relatively limited, just 20 (4.5%). Of this number, 17 were assigned an As or A rank, having suffered a quick brittle fracture. Three other piers were given a rank of B1 or below and had visible damage characteristics; these are shown in Table 3. The main characteristic of these piers was that their crack inclination angle was steeper than 45°. This is because their hoop-tie ratio was smaller than the main reinforcement ratio, as indicated in Reference 4.

The cracking of the three piers was grouped into two types: one was the type in which cracking propagated to a degree of about 70° after originating from the intersection of a beam and a column, as shown by the left-hand sketch in Fig. 5. When this cracking continued, the beam and the main reinforcement in the column were torn, as seen in the right-hand sketch in the figure. One reason for this damage was that the number of hoop ties, which were arranged around the main reinforcements in the beam, was not sufficient in quantity. The other cracking type was shear cracking, which propagated at a degree of about 60 ° after starting from somewhere between the bottom and the mid-height of the column, as shown by the left-hand sketch in Fig. 6. Characteristic of this cracking is that it started near the ground surface of the column. When this cracking continued, it resulted in typical shear damage at the column's mid-height, as seen on the right in Fig. 6. Both of these types of damage are considered due to an insufficient number of hoop ties around the main reinforcement.

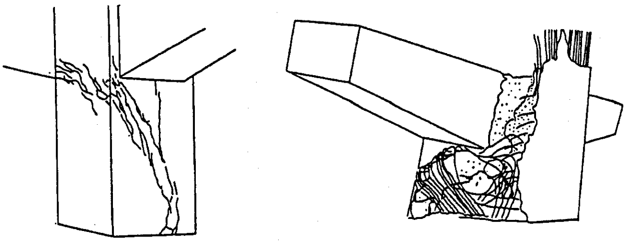

Fig.5 Damage pattern (left : cracking right : fracture)

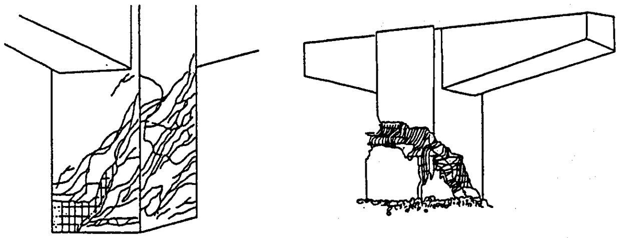

Fig.6 Damage pattern (left : cracking right : fracture)

4.2 Effect of reinforcement termination

The positions of reinforcement termination in the actual piers were confirmed utilizing detailed damage sketches, photos, and the original bar arrangement drawings used at the time of bridge construction. Table 4 shows the relationship between the presence or absence of reinforcement termination and the damage types. Of the 278 piers without reinforcement termination, 234 (84%) were damaged at the pier bottom by flexure or flexural shearing. The remaining 44 were damaged by shearing or flexural shearing at the column's mid-height. This is because the resistivity of the column's cross-section to an acting shear force is sometimes smaller at the column's mid-height than at the column's bottom because of the effect of a/d (shear span ratio).

Table 5 shows the relationship between the presence or absence of reinforcement termination and the damage levels. Of the 95 piers without reinforcement termination that suffered damage of B1 level or higher, 13 were damaged at the mid-height of the column. Actually, 11 of them were of As and A damage rank. They were the piers with a large square cross-section that were located at the crossings of ground-level roads. Of the 287 piers without reinforcement termination that suffered damage of various ranks, 234 were damaged by flexure at the column bottom. Of the 82 piers ranked B1 or above, 52 were damaged by flexural shearing.

Table 4 Termination of reinforcement and types of pier damage

			Damage type			Total
			Flexural	Flexural shear	shear	
Reinforcement terminated	Positions of damage	Mid-height	19	83	3	105
		Bottom	41	4	0	45
	Total		60	87	3	150
Reinforcement not terminated	Positions of damage	Mid-height	0	30	14	44
		Bottom	158	73	3	234
	Total		158	103	17	278

Table 5 Termination of reinforcement and damege ranking of piers

			Damage rank			Total
			A·As·B1	B2·B3	C1·C2·D	
Reinforcement terminated	Positions of damage	Mid-height	71	4	36	111
		Bottom	2	9	34	45
	Total		73	13	70	156
Reinforcement not terminated	Positions of damage	Mid-height	13	2	38	53
		Bottom	82	37	115	234
	Total		95	39	153	287

15 piers without damage were excluded

Figure 7 shows the distribution of damage to piers with reinforcement termination. Figure 8 shows the same distribution, but to piers without reinforcement termination. With regard to the former type of piers, about half of them were of As or A damage rank and the remaining half were mostly C-rank or below, with a few piers suffering intermediate level of damage of B1, B2, or B3 rank. This means that piers with reinforcement termination tend to cause shear-type damage at the termination point, and once damage is triggered, the damage quickly develops into major damage. In contrast, the damage distribution of piers without reinforcement termination is scattered, as seen from Fig. 8. This is because they tended to suffer flexural damage at the bottom of the column. Therefore, it can be said that the presence or absence of reinforcement termination had a significant effect on the damage level, the damage type, and the location of the damage to piers.

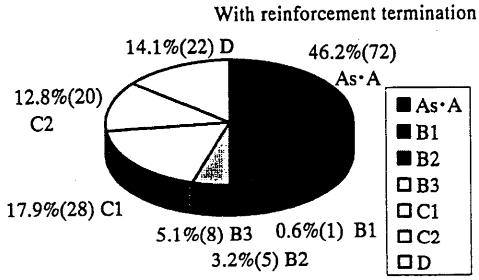

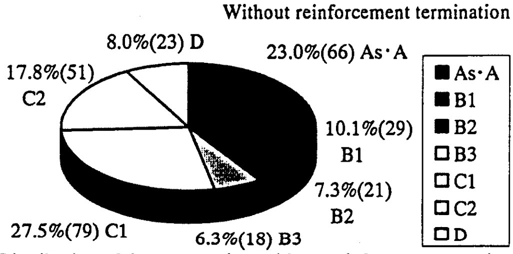

Fig.8 Distribution of damage to piers without reinforcement termination

Fig.7 Distribution of damage to piers with reinforcement termination

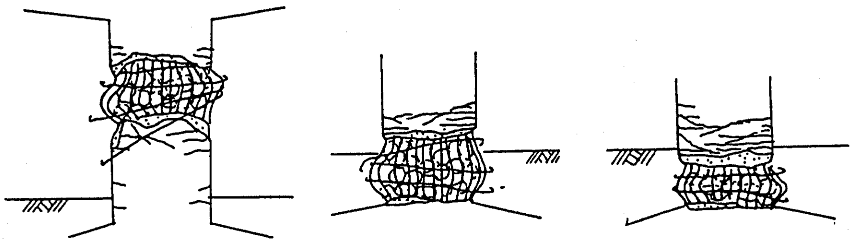

(a) Column mid-height (b) Near ground surface (c) Underground

Fig.9 Positions of pier damage

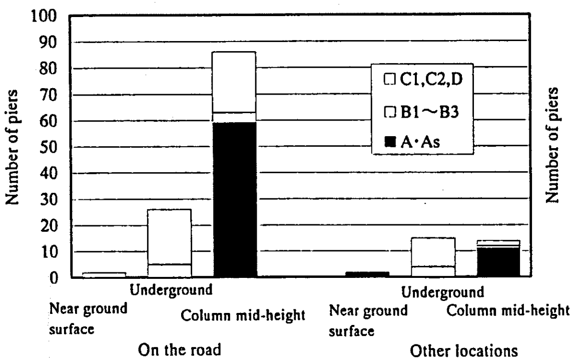

Fig.10 Damage ranking and damage positions of piers with reinforcement termination

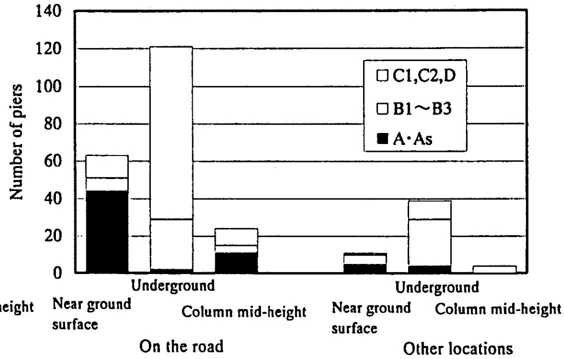

Fig.11 Damage ranking and damage positions of piers without reinforcement termination

4.3 Locations of damage

To investigate the effect of the locations of the damage, the locations of the damage to the piers were grouped into three types: underground, near the ground surface, and at the column's mid-height. These groups are shown in Fig. 9. Here, the position "underground" means predominant damage occurred in the underground section of the column and the damage was not observable from the surface. The position "near the ground surface" means the dominant damage was near the ground surface of the column. The backfill depth at the column bottom averaged 1.5 m.

Figures 10 and 11 show the locations of damage to piers with and without reinforcement termination, respectively, and grouped by pier location, either on a ground-level road or other locations. Figure 10 shows that major damage to the piers occurred mostly at the mid-height of the columns, and that damage near the ground surface was very limited. The location of the damage and the damage rank did not differ much in this type of pier, regardless of their locations (either on a ground-level road or other locations). In contrast, piers without reinforcement termination suffered relatively low-level damage when the piers were at other locations, but when piers were on a ground-level road, many of them suffered damage to the column near the ground surface, and their damage levels tended to be higher, even though their reinforcement was not terminated, as seen from Fig. 11. This is probably because seismic motion was very severe locally and the column bottom was confined due to the effect of ground conditions, such as pavement. The effect of these ground conditions will be examined in detail in Section 5.

4.4 Strength of piers ranked As and A

a) Piers with reinforcement termination

The cause of the damage to As- and A- ranked piers on the Kobe Route were analyzed. Table 6 is a breakdown of the damage to the piers. Piers with reinforcement termination totaled 72 and those without reinforcement termination totaled 66. Of the 72 with reinforcement termination, 70 were damaged at the mid-height of the column. Comparing the damaged piers with their bar arrangement drawings, it was found that the locations of the damage corresponded to the points of reinforcement termination. With regard to the two piers damaged near the ground surface, their damage also corresponded to the reinforcement termination points, as drawings indicated that the reinforcement was terminated 2 m from the column bottoms. The relationship between the shear strength index (α_{su}) and the yield flexural strength index (α_{my}) for the 72 piers is shown in Fig. 12. The values of α_{su} and α_{my} are expressed by the following equations:

$$\alpha_{su} = 980 \cdot Su / (Wu + Wp)$$
$$\alpha_{my} = 980\,(My - Mo) \,/\, (Wu + 0.5Wp) \cdot la \qquad \text{............} \quad (1)$$

where,

α_{su} : shear strength index (gal)
Su : shear strength derived from the 1990 Specifications for Highway Bridges (tf)
Wu: weight of the superstructure carried by the pier (tf or kN)
Wp: weight of the pier (tf or kN)
α_{my} : yield flexural strength index (gal)
My : bending moment at the time when the outermost reinforcement reaches the yield stress on the cross-section to which constant axial force acts (tf・m or kN・m), which is derived by the 1990 Specifications for Highway Bridges
la : distance from cross-section of the focus to the point at which the inertial force is imposed by the superstructure (m)
Mo: Eccentric bending moment (tf or kN)

Table 6 Termination of reinforcement and positions of damage to piers with As and A ranks

Reinforcement	Locations of piers	Positions of damage	Number of piers		
Reinforcement terminated	On the Road	Mid-height	59	59	72
		Near ground surface	0		
		Underground	0		
	Other locations	Mid-height	11	13	
		Near ground surface	2		
		Underground	0		
Reinforcement not terminated	On the Road	Mid-height	11	57	66
		Near ground surface	44		
		Underground	2		
	Other locations	Mid-height	0	9	
		Near ground surface	5		
		Underground	4		

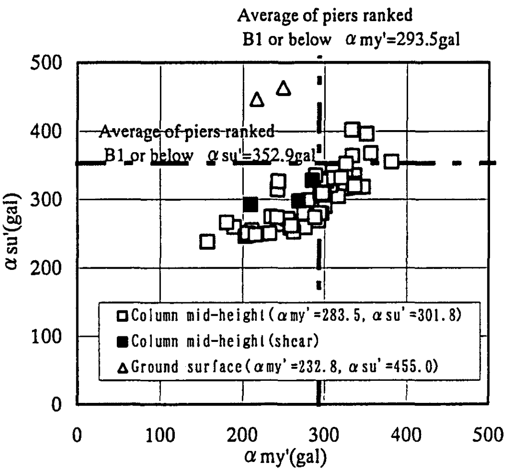

Fig.12 Relationship between shear index and yield flexural index

The average shear strength index of the 72 piers, or 306 gal, was much smaller than the 353 gal derived from the piers of B1 rank or below. Two piers that suffered damage near the ground surface had a relatively large shear strength index of 450 gal because their reinforcement reduction from 2 layers to 1.5 layers did not cause any significant decline in their shear strength, but their yield flexural strength index was as small as 200 ~ 250 gal. Therefore, it is assumed that the flexural cracks at the point of reinforcement termination near the column bottom continued to propagate, leading to severe damage from flexural shearing [5].

All the piers with reinforcement termination that were ranked As and A were damaged at the point of termination. Though the damage levels differed slightly, the severe damage was caused because the flexural and shear strengths at the point of reinforcement termination were comparatively smaller than at other points.

b) Piers without reinforcement termination
Of the 66 piers without reinforcement termination, 11 were damaged at the mid-height of the columns and 55 at the bottom of the columns (near the ground surface and underground). The 11 were all large piers with a square cross-section constructed at the crossings of ground level roads. To support their large dead loads, the cross-sectional width is large and the a/d comparatively small. Figures 13 and 14 show the relationship between the flexural strength and shear strength of piers without reinforcement termination, and the relationship between the yield flexural strength index and shear strength index, respectively.

As seen from the figures, the ratio of shear strength to flexural strength of the piers that suffered damage at the mid-height of the columns was below 1, and the average shear strength index of those piers, 327 gal, was smaller than the average shear strength index of the piers of B1 rank or below, which was 397 gal. This indicates that piers with a small shear strength/flexural strength ratio and piers with extremely low shear strength tend to be damaged by shearing at the mid-height of the column rather than at the bottom. These results suggest that sufficient shear strength, and an additional margin for safety, should be provided not only at the bottom area of the column but also at mid-height. Piers without reinforcement termination that were damaged near the bottom and underground had an average shear strength of 360 gal and 387 gal, respectively, which was slightly smaller than the 397 gal for piers of B1 rank or below. The yield flexural strength index of the piers was widely scattered and no qualitative tendency was found.

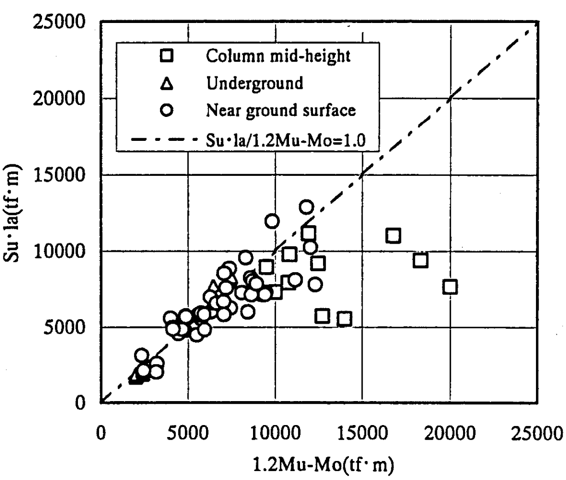

Fig.13 Relationship between shear capacity and flexural capacity

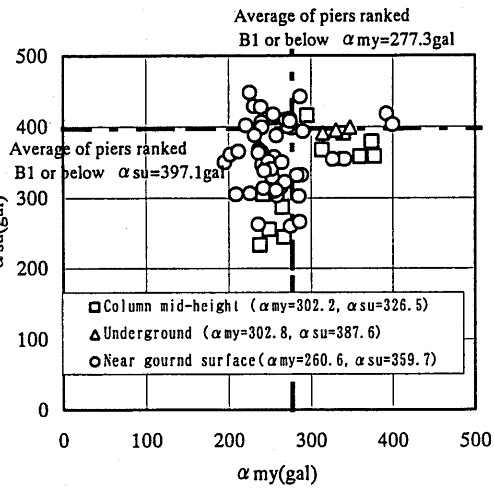

Fig.14 Relationship between shear index and yield flexural index

5. ANALYSIS OF GROUND RESISTANCE

5.1 Outline of analysis

a) Piers for analysis
As already seen from Tables 4 and 5, many piers were found to be damaged near the bottom (near the ground surface and underground). The effect of ground resistance on the damage level of the piers was analyzed by two-dimensional nonlinear FEM analysis. Details of the analytical procedure are given in Reference 6. Selected for analysis was an actual T-shaped RC pier, the configuration, of which is shown in Fig. 15. The pier has a

circular cross-section, 3.5 m in diameter, a height of 12.66 m, and supports a steel I-shaped simple girder that has spans of 60 m and 39 m. The 1/5 of the reinforcements is terminated at a height 6.45 m from the upper face of the footing. The backfill depth is 1.5 m. Of this length, 0.5 m is concrete pavement and 1.0 m is earth with an N value of 15.

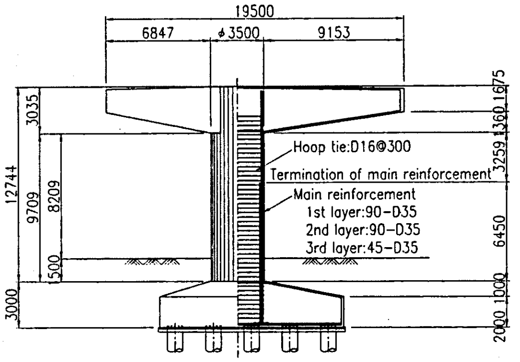

Fig.15 Configurations of a pier for analysis and its reinforcement arrangement

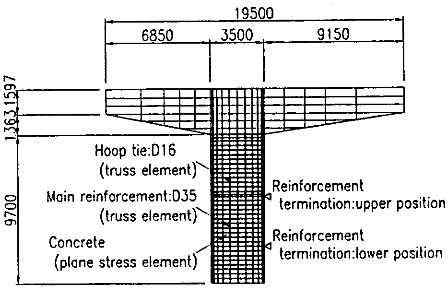

Fig.17 Analysis model

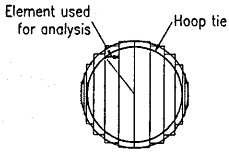

Fig.16 Element used for analysis as a hoop tie

Table 7 Physical properties

	Concrete	Reinforcement
Young's modulus(N/mm^2)	2.59×10^4	2.59×10^4
Poisson's ratio	0.167	0.300
Compressive strength(N/mm^2)	35.2	—
Tensile strength(N/mm^2)	2.5*	—
Yield strength(N/mm^2)	—	349.1

* Determined based on the Specification for Highway Bridges[3]

b) Analytical model

The section of the pier above the footing's upper face was selected for analysis. Focus was on the direction perpendicular to the bridge axis. The bottom of the column was assumed to be fixed. The pier was modeled two dimensionally. The concrete of the pier was assumed to be a plane stress element and the reinforcement a truss element. As parameters, the point of reinforcement termination and the ground resistance were selected. The model was constructed based on the following conditions:

① Two positions were assumed as the reinforcement termination points:

<Upper termination point>

The upper reinforcement termination point was set at 5.65 m from the upper face of the footing by deducting the anchoring length of 80 cm specified by the Concrete Specifications from 6.45 m, which is the reinforcement termination point of the actual piers.

<Lower termination point>

The lower reinforcement termination point was set at 2.4 m from the upper face of the footing by deducting the anchoring length of 80 cm from 3.2 m, which is 1/2 of 6.45 m.

② Hoop ties

As the model was two dimensional, the effect of the hoop ties was taken into consideration by converting the hoop tie ratio into the area of the inplane element, as shown in Fig. 16.

③ Ground resistance by backfill

This was considered to be an elastic spring, and the spring value was determined based on the Specifications for Highway Bridges.

The derived analysis model, constructed of two dimensional finite elements based on the above conditions, is shown in Fig. 17.

c) Physical properties of analysis model

The physical properties of the analysis model were determined as described in Table 7 and based on the results of a laboratory test conducted on samples taken from actual piers. The following models were used to account for the nonlinear characteristics of the analysis model.

① Stress-strain relationship under compressive force : Saenz model
② Strain softening characteristic under compressive force : Darwin-Pecknold model
③ Shear transfer after cracking : Al-Mahaidi model
④ Reinforcement : bilinear model

d) Loading condition

Loading was applied to the nodal points of the main girders, producing displacements up to 50 cm after analysis under the dead weight condition was conducted.

5.2 Analytical results

a) Case 1: ground resistance is not considered

The load-displacement relationship is shown in Fig. 18. The maximum load was 8.96×10^6N when the main reinforcement was terminated on the upper side of the column, and 8.81×10^6N when it was terminated on the lower side of the column. The analytical load-displacement relationship is roughly in agreement with the flexural strength derived from the Specifications for Highway Bridges, which is also shown in the figure. Figure 19 shows the distribution of vertical strain and shear strain at the time of $7\delta_y$ (δ_y: displacement when the main reinforcement within the 45° of the tensile side of the cross section buckled).

When the main reinforcement was terminated on the upper side, the piers failed at the bottom of the columns as the vertical and shear strain areas were enlarged at those locations. In contrast, when the termination point was on the lower side, the piers failed at both the bottom and at the reinforcement termination point after the vertical strain area was enlarged at those two locations and the shear strain area propagated from the reinforcement termination point toward the bottom of the column.

b) Case 2 : ground resistance is considered

The load-displacement relationship for Case 2 is shown in Fig. 20. The maximum load was 9.82×10^6N when the reinforcement was terminated on the upper side of the column, and 9.43×10^6N when it was terminated on the lower side of the column. Both values are greater than those of Case 1. Figure 21 shows the distributions of vertical strain and shear strain at the time of the displacement of $7\delta_y$. When the reinforcement termination point was on the upper side, the vertical strain area was enlarged on the column near the surface of the backfill and the shear strain area was concentrated in the area between the surface of the backfill and the reinforcement termination point. Though the flexural capacity was increased by about 10% because the flexural span was shortened due to ground resistance, the shear failure mode was apparently enhanced on the pier by the dominating area of shear strain near the ground surface.

5.3 Discussion

When designing a pier, the ground resistance around the pier is usually excluded from consideration so as to increase the safety of the pier. However, if the physical condition near the ground surface is rocky due to the presence of concrete, the shear fracture mode will be enhanced on the pier and will likely cause a brittle fracture. Because of this, the deformation capacity of the pier will decline, even though flexural strength is increased. This is probably why shear damage and flexural shear damage are often found near the ground surface of the column. Therefore, sufficient shear strength should be provided in this area of the column in order to avoid shear failure.

6. DAMAGE TYPES AT REINFORCEMENT TERMINATION POINTS

As stated earlier, damage to the piers varied widely, depending on the presence or absence of reinforcement termination. Damage analysis was conducted focusing on piers with reinforcement termination. Figure 22 shows the relationship between the yield flexural strength index (α_{my}) and the actual damage to the piers. As seen from the figure, those piers which were damaged at the bottom of the column all had a considerably greater α_{my} value at the reinforcement termination point than at the bottom of the column and, therefore, the

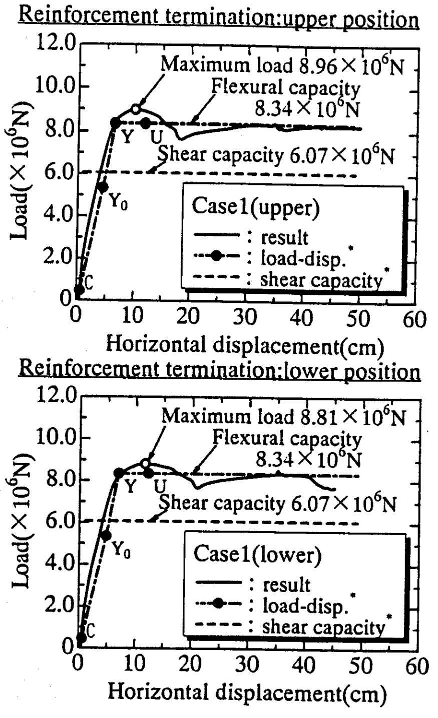

* Spec. of Highway Bridges

Fig.18 Load-displacement relationship(Case1)

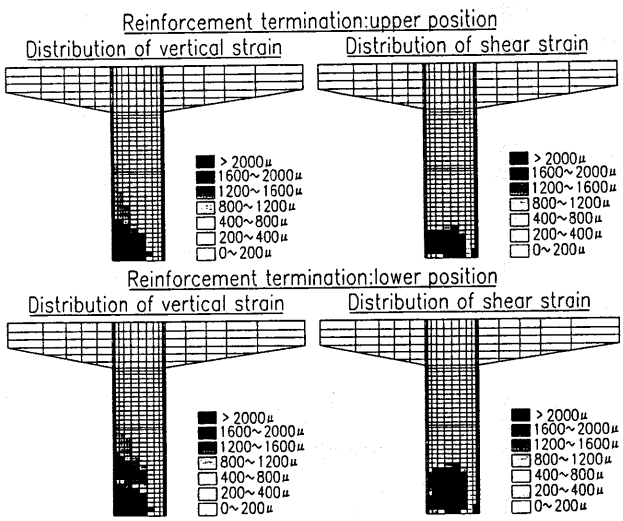

Fig.19 Distribution of strain(Case1)

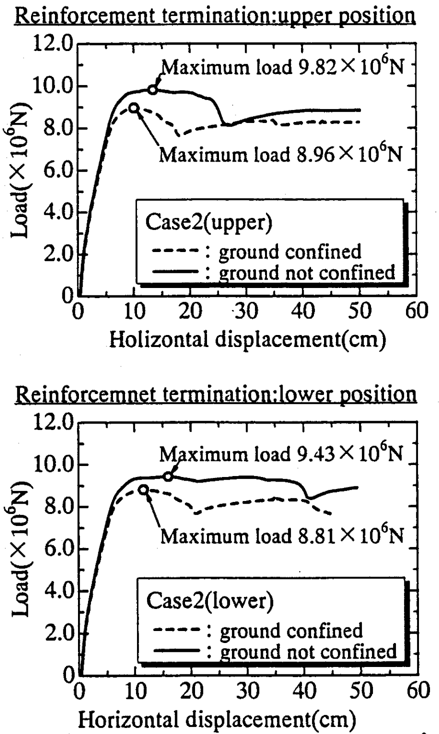

(case 2)

Fig.20 Load-displacement relationship

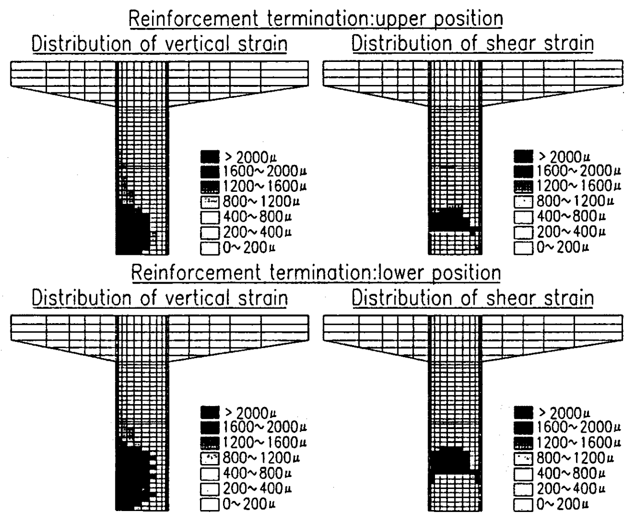

Fig.21 Distribution of strain(Case2)

damage preceded from the latter position. There were also many other piers which suffered damage at the termination point, even though the value of α_{my} at that position was greater than at the bottom of the column. The α_{my} value at the termination point of these piers was relatively small compared to that of piers that had failed at the bottom of the columns. Also, most piers damaged at the bottom had failed due to flexure, but piers damaged at the reinforcement termination point mostly failed due to flexural shearing. The α_{my} value, or yield flexural strength index, is an index that causes a yield bending moment on the cross-section of the focus. It is calculated by Equation (2).

$$\alpha_{my} = My / (W \cdot 1a) \qquad \text{...............} \quad (2)$$

where,

1a : distance from the cross-section of the focus to the point at which the inertial force is imposed from the superstructure (m)

W : weight contributing to flexure of the column above the cross-section of the focus (tf)

Figure 23 shows the values of α_{my} and $\alpha_{my'}$, which are yield flexural strength indices (gal) at the bottom of the column and the reinforcement termination point, respectively. The marks in the figure are gathered into two groups: ranks A and B, and ranks B2, B3, C, and D. As seen from the figure, the damage level is higher for small piers with a gal of below 350 at both the bottom of the column and the reinforcement termination point. Also, a correlation is seen between the damage level, the shear strength index, and the yield flexural strength index. It is also seen that piers with a relatively large $\alpha_{my'} / \alpha_{my}$ ratio at the reinforcement termination point and in the bottom area around the column suffered comparatively little damage. This is probably due to the fact that the reinforcement termination in those piers did not become a vulnerable point and hence the bottoms of the columns suffered minor flexural damage.

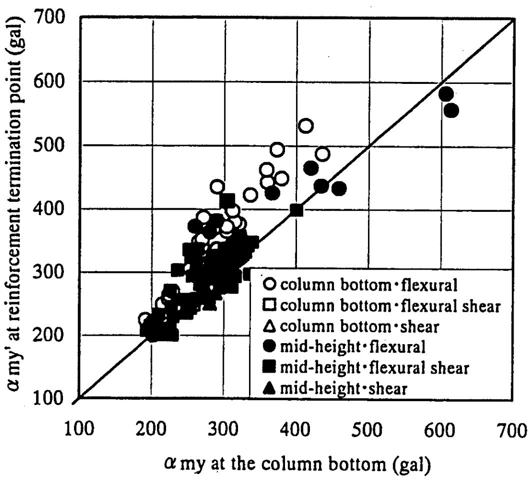

Fig.22 Relationship between yield flexural index and damage positions

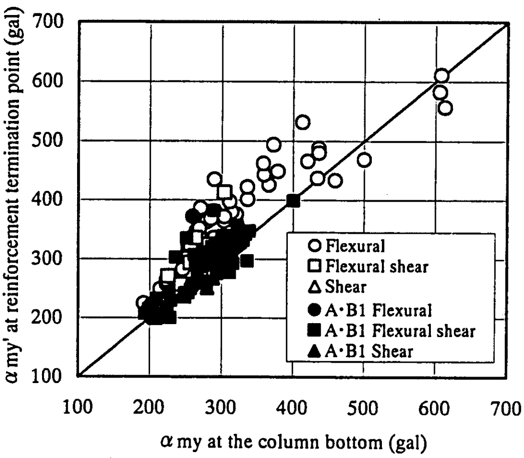

Fig.23 Relationship between yield flexural index and damage ranks

7. CONCLUSIONS

A detailed damage assessment was conducted on the RC single piers on the Hanshin Expressway Kobe Route, which suffered damage in the 1995 Hyogoken-Nambu Earthquake. The following conclusions were drawn from the results:

① Based on the results of a detailed damage assessment, many piers ranked C and D in the first-round visual inspection were given a B rank, which required their reinforcements to be replaced. This is primarily because damage to the columns below the ground was newly found.

② It was found by the detailed investigation of the damage levels that the length of the buckling of the main reinforcement was slightly smaller than the width of the column cross-section if the cross-section was over 200 cm, as was the case with the actual piers.

③ Piers with reinforcement termination mostly suffered damage of As and A ranks and few suffered B rank damage. This is because the damage at the reinforcement termination point propagated quickly and ended in severe damage.

④ Of the 138 piers ranked As and A, 72 had reinforcement termination and 66 did not. The 72 piers with reinforcement termination failed at the termination point. Their shear strength index, 306 gal, was significantly smaller than that of piers of B1 rank or below, which had a shear strength index of 353 gal.

⑤ The 11 piers of As and A ranks, which suffered damage at the mid-height of the column even though they did not have reinforcement termination at that point had a shear strength/flexural strength ratio of below 1, and their average shear strength index, 327 gal, was smaller than that for piers below B1 rank, which was 397 gal. The 55 piers which suffered damage near the ground surface and underground had a relatively small shear strength index of 363 gal.

⑥ If the shear strength index of the pier was below 400 gal, the damage level tended to be more severe regardless of the presence or absence of reinforcement termination. This suggests that piers with a small shear strength index value need to be strengthened.

⑦ Piers without reinforcement termination and situated on a ground level road were mostly damaged near the ground surface, and their damage level tended to be higher. According to the two-dimensional nonlinear FEM analysis, if the ground surface is very hard, the shear fracture mode is enhanced and damage occurs at the bottom of the column. Therefore, sufficient shear strength should be provided to the bottom of the column near the ground surface.

REFERENCES

[1] Road Association of Japan, "Handbook for Roads Damaged by Earthquakes: Retrofit Procedure", 1988.2 (in Japanese)

[2] Shimpo, H., Murayama, Y., and Suda, K., "Experimental Study on Buckling of Main Reinforcement in RC Columns", Proc. of 49th Annual Conference of JSCE, V-5, pp. 966-967, 1994.9 (in Japanese)

[3] Yokoi, K., Fujii, M., Yasuda. F., and Kosa, K., "Experimental Study on Seismic Strengthening Effect of Damaged RC Piers", Proc. of JCI, Vol. 18, No. 2, pp.137-142, 1996 (in Japanese)

[4] Mizuta, T., Kobayashi, K., Kosa, K., and Yasuda, F., "Evaluation of Shear Strength of RC Piers in Existing Bridges Using Modified Compression Field Theory", Proc. of JCI, Vol. 19, No. 1, pp.387-392, 1997 (in Japanese)

[5] Kosa, K., Fujii, M., Hayashi, H., and Nakata, T., "Evaluation of Earthquake-Damaged RC Piers by the Ultimate Bearing Capacity Procedure", Proc. of JSCE, No.592/V-39, pp.73-82, 1998.5 (in Japanese)

[6] Ouchi, H., Hayashi, H., Kosa, K, and Tasaka, M., "A Numerical Study on Bridge Column Damage due to Seismic Actions", Proc. of JCI, Vol. 19, No. 2, pp.411-416, 1997 (in Japanese)

[7] Ishibashi, T., "Damage to RC Viaducts for Railway and Their Design Earthquake Resistance", Concrete Journal, JCI, Vol.34, No.11, pp.56-58, 1996.11 (in Japanese)

[8] Abe, S., Fujino, Y., Abe, M., "An Analysis of Damage to Hanshin Expressway During 1995 Hyogoken-Nambu Earthquake" Proc. of JSCE, No.612/I-46, pp.181-199, 1999.1 (in Japanese)